# Structure and characterization of the glycan moiety of L-amino-acid oxidase from the Malayan pit viper *Calloselasma rhodostoma*

**Armin Geyer[1], Teresa B. Fitzpatrick[2], Peter D. Pawelek[3], Karina Kitzing[2], Alice Vrielink[3], Sandro Ghisla[1] and Peter Macheroux[2]**

[1]*Section of Natural Sciences, Universität Konstanz, Germany;* [2]*Institute of Plant Sciences, Swiss Federal Institute of Technology Zürich, Zürich, Switzerland;* [3]*Biochemistry Department, McIntyre Medical Sciences Building, McGill University, Montreal, Québec, Canada*

Ophidian L-amino-acid oxidase (L-amino-acid oxygen:oxido-reductase, deaminating, EC 1.4.3.2) is found in the venom of many poisonous snakes (crotalids, elapids and viperids). This FAD-dependent glycoprotein has been studied from several snake species (e.g. *Crotalus adamanteus*, *Crotalus atrox* and *Calloselasma rhodostoma*) in detail with regard to the biochemical and enzymatic properties. The nature of glycosylation, however, as well as the chemical structure(s) of the attached oligosaccharide(s) are unknown. In view of the putative involvement of the glycan moiety in the biological effects of ophidian L-amino-acid oxidase, notably the apoptotic activity of the enzyme, structural knowledge is needed to evaluate its exact function. In this study we report on the glycosylation of L-amino-acid oxidase from the venom of the Malayan pit viper (*Calloselasma rhodostoma*). Its glycosylation is remarkably homogenous with the major oligosaccharide accounting for approximately 90% of the total sugar content. Based on detailed analysis of the isolated oligosaccharide by 2D NMR spectroscopies and MALDI-TOF mass spectrometry the glycan is identified as a bis-sialylated, biantennary, core-fucosylated dodecasaccharide. The biological significance of this finding is discussed in light of the biological activities of the enzyme.

*Keywords*: L-amino-acid oxidase; flavoprotein; snake venom; glycosylation; structure of glycan moiety.

The flavoprotein L-amino-acid oxidase (LAAO) which catalyses the transformation of L-amino acids to the corresponding α-keto acids with the concomitant release of hydrogen peroxide and ammonia is a constituent of snake venom (Scheme 1). The enzyme is found in most venomous snakes and contributes to the toxicity of the venom [1]. The toxicity is in part due to impairment of platelet aggregation, which enhances the observed injuries in snake bite victims [2,3]. As first shown in 1969 for LAAO from *Crotalus adamanteus* the majority of the protein components of snake venom are glycosylated [4]. In this context it is interesting to note that while ophidian LAAO was reported to exhibit an antibacterial activity this was not observed with the closely related flavoenzyme D-amino-acid oxidase [5,6] in spite of the latter forming identical products, i.e. an α-keto acid, hydrogen peroxide

and ammonia. In contrast to the ophidian LAAO, however, D-amino-acid oxidase is not glycosylated. This suggests that glycosylation is a feature required for this antibacterial effect. More recently it was reported that LAAO (apoxin I) from *Crotalus atrox* (Western diamondback rattlesnake) possesses apoptosis-inducing activity *in vitro* and *in vivo* [7–10]. Based on fluorescence labelling studies it was suggested that LAAO docks to the cell surface leading to the generation of high local concentrations of hydrogen peroxide [7,8]. This in turn may lead to oxidative damage of the cell precipitating an apoptotic response. It is also interesting to note that the LAAO-induced apoptosis has been reported to be distinct from that caused by exogenous hydrogen peroxide suggesting that the mode of delivery of hydrogen peroxide is an important factor [7,8]. The role of the glycosyl substituent(s) for these interesting biological activities remains to be elucidated.

While the reaction mechanism and the unusual freeze- and pH-induced reversible inactivation of this enzyme have been studied (reviewed in [11]), the role(s) and the chemical structure of the glycan including its mode of attachment to the protein has received little attention. A first attempt to quantitate the sugar composition was undertaken by deKok and Rawitch [12] with *C. adamanteus* LAAO who established the presence of fucose, mannose, galactose (*N*-acetyl)glucosamine and sialic acid as constituents of the oligosaccharide moiety. It was also shown that glycosylation contributes to the microheterogeneity reported for LAAO [4]. In order to pave the way for a detailed analysis of its involvement and significance in the mentioned biological effects we have recently cloned the cDNA of LAAO from *Calloselasma rhodostoma*, the Malayan pit viper, deduced the amino-acid sequence (Genbank accession

**Scheme 1. Reaction catalyzed by LAAO.**
Note that subsequent to dehydrogenation, the formed imino acid is hydrolyzed to the final products (in brackets). Whether the latter step is catalyzed by the enzyme or occurs spontaneously has not yet been clarified.
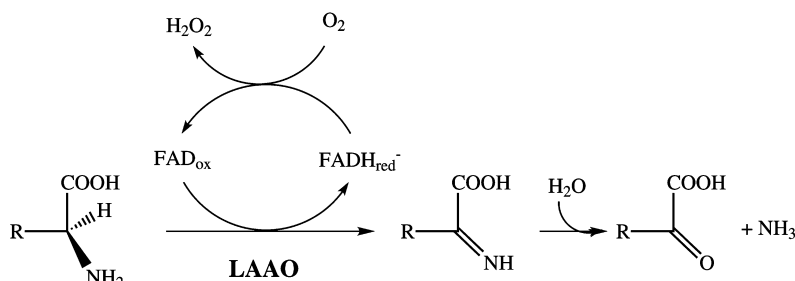
number: AJ271725), and determined the X-ray structure of the native protein [13]. This enzyme exhibits two putative N-glycosylation consensus motifs, one, at Asn361, is conserved in LAAOs from *C. adamanteus* and *C. atrox* (the two other ophidian LAAOs for which the amino-acid sequence is known). The other possible N-glycosylation site at Asn172 is unique to *C. rhodostoma* LAAO [14]. The three-dimensional structure of *C. rhodostoma* LAAO shows that both sites are glycosylated in the native protein [13] with the site at Asn172 carrying a fucosylated *N*-acetylglucosamine. Owing to the high flexibility of the glycan moiety, X-ray structural analysis revealed only the structure of the proximal residues of the glycan moiety. In view of the relevance of the oligosaccharide moiety of LAAO, we have analyzed the glycosylation of LAAO, isolated the glycan moiety and elucidated the entire oligosaccharide structure by 2D NMR spectroscopy and mass spectrometry.

# EXPERIMENTAL PROCEDURES

## General chemicals

2,4-Dihydroxybenzoic acid (DHB), 2′,4′,6′-trihydroxy-acetophenone (THAP), periodic acid and sodium metabisulfite were from Fluka, Buchs, Switzerland. Schiff's reagent was from Sigma, Poole, Dorset, UK. All other chemicals were of the best available grade.

## Enzymes

L-Amino-acid oxidase was obtained from the venom of the Malayan pit viper (*Calloselasma rhodostoma*) as described [14]. LAAO-containing side fractions from purification of Ancrod were generously supplied by M. Kurfürst, Knoll AG, Ludwigshafen, Germany. This LAAO preparation had an $A_{272}/A_{460}$ ratio of 9 : 1 and did not show contaminating proteins on SDS/PAGE, so is therefore assumed to be > 98% pure. All operations were carried out in 100 mM Tris/phosphate buffer, pH 8.0. Endo $H_f$, peptide:*N*-glycosidase F (PNGase F) and *N*-acetylneuraminyl hydrolase (sialidase) were from New England Biolabs. *O*-Glycosidase was from Boehringer Mannheim, Germany.

## General methods

Polyacrylamide gel electrophoresis (10% SDS) was performed according to Laemmli [15]. Detection of protein glycosylation was performed with Schiff's reagent as described previously [16].

## Fluorophore-assisted carbohydrate electrophoresis (FACE)

Chemical labelling with 8-aminonaphthalene-1,3,6-trisulfonic acid (ANTS) of oligosaccharides released from LAAO by PNGase F was carried out with the N-linked oligosaccharide profiling kit from BioRad (catalog no. 170-6501). All operations were performed as described in the manual provided by the manufacturer.

## Preparation and purification of oligosaccharides

The glycan moiety was released from native LAAO by treatment with PNGase F, using the experimental conditions recommended by the manufacturer (New England Biolabs). For the preparation of samples used in NMR investigations the surfactants recommended by the manufacturer were omitted from the incubation as these interfere with the NMR measurements and are difficult to separate from the sugar moiety. Purification was thus carried out as follows: 60–80 mg LAAO in 4.5 mL 0.1 M Tris/sodium phosphate buffer, pH 8 were incubated with PNGaseF (50 000 U) overnight at 37 °C. The colorless protein precipitate was removed by centrifugation (15 mins at 16 000 *g*), the supernatant was filtered through a Centriprep 30 membrane, and then the retardate washed three times with 0.5 mL distilled water. The combined filtrates were then lyophilized, and the residue was chromatographed over a Sep-Pak column (2 g, Waters). The column was washed with 5 mL distilled water and the oligosaccharide eluted with 5 mL methanol. The pooled methanol eluates were concentrated to dryness and redissolved in $D_2O$ for NMR measurements.

## Mass spectrometry

Protein samples for ESI-MS were desalted before use with a Resource RPC column (3 mL bed volume, Pharmacia). The protein was eluted from this column with a linear gradient of 0.1% trifluoroacetic acid in water (v/v) to 0.1% trifluoroacetic acid in acetonitrile (v/v) at a flow rate of 3 mL·min$^{-1}$. The fraction containing the protein was collected and then lyophilized (or dried in a speed-vac apparatus). The desalted LAAO was dissolved in 2 μL 70% (v/v) formic acid, which was then diluted 20-fold with 50% methanol. ESI-MS was then carried out with a Finnigan Mat (San Jose, CA, USA) LCQ ion trap mass spectrometer. Samples (2 μL) were introduced by flow injection with a mobile phase of 50% methanol, 1% formic acid in water (v/v). Capillary voltage was 2.2 kV and the flow rate was

0.5 μL·min$^{-1}$. Mass spectra of multiply charged species were acquired in the range 500–2000 a.m.u. and deconvoluted to yield the native polypeptide mass using software provided by the manufacturer. The error of the mass determination was estimated to be 0.02%, i.e. approximately 10 Da in the mass range of interest.
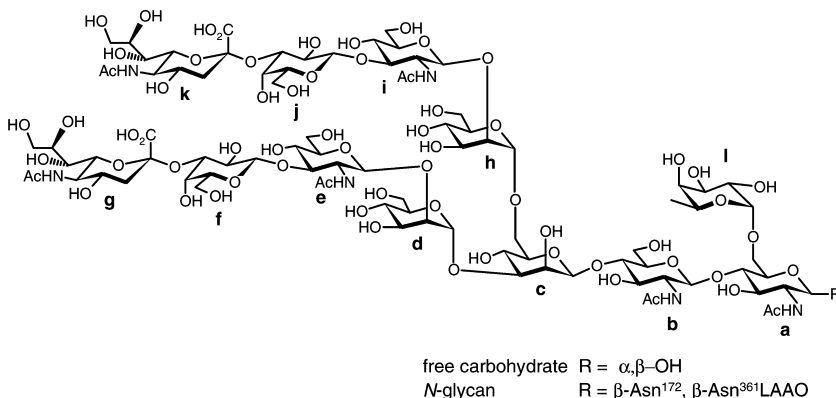
MALDI-TOF mass spectra were recorded with a Voyager Elite biospectrometry research station (PerSeptive Biosystems, Framingham, MA, USA). The oligosaccharide was released with PNGase F from LAAO and then directly analyzed by mass spectrometry without further purification. THAP was used as matrix and sample preparation was carried out as described in [17]. The spectrometer was operated in the negative ion, linear mode using an accelerating voltage of 25 000 V. Under these operating conditions, the error of mass determination is approximately 0.05%.

### NMR-spectroscopy

NMR spectra were acquired with a Bruker DRX 600 spectrometer at 303 K and chemical shifts were calibrated to the sodium salt of trimethylsilylpropionic acid. Proton spin systems were assigned by TOCSY [18] and COSY [19]. $^{13}$C chemical shifts were identified by HMQC [20]. ROESY was used to identify short interproton distances [21,22]. The mixing time was 200 ms. All 2D experiments were recorded in the phase-sensitive mode by using time-proportional phase incrementation. Data matrices contained 2K points in f2 and 512 points in f1. For data processing the matrices were zero-filled to 1K data points in f1 and apodized with a squared sine bell function shifted by π/2 in both dimensions.

### Modeling and energy minimization

The atom positions of the dodecasaccharide depicted in (Scheme 2) were obtained after energy minimization with the force field MM+ (HYPERCHEM program package, Hypercube Inc., Waterloo, Ontario, Canada). Glycosidic torsions were oriented to the syn conformation, as determined for similar N-glycans [23]. Four dodecasaccharide moieties, two for each protein monomer, were linked to the Asn glycosylation sites identified in the 3D-structure [13].

### Isoelectric focusing

Isoelectric focusing was carried out on a Multiphor II electrophoresis unit using the Immobiline DryStrip kit (Amersham Pharmacia Biotech). The method was carried out as described by the manufacturer employing 18 cm pH 4–7 L IPG strips. Protein samples (60 μg) were included in the IPG strip rehydration solution (8 M urea, 2% Chaps, 2% pH 4–7 IPG buffer, 18 mM DTE, trace of Bromophenol blue). Focusing was achieved using a tri-phase programme of 500 V for 1 min, followed by a gradient of 500–3500 V for 1.5 h and finally maintaining the voltage at 3500 V for 17 h, respectively. Bands were visualized using Coomassie blue staining.

## RESULTS

### Mass determination and electrophoretic properties of L-amino-acid oxidase

The molecular mass of native, purified LAAO from *Calloselasma rhodostoma* as determined by means of electrospray-ionization mass spectrometry is 59968 Da (Fig. 1). This mass is ≈ 3700 Da higher than the mass predicted from the primary amino-acid sequence (56234 Da). Untreated protein appears as a single band with an apparent molecular mass of 58 kDa in SDS gel electrophoresis (Fig. 2A, lane 1). The native protein also stains with Schiff's reagent demonstrating that it is glycosylated (Fig. 2B, lane 1). Treatment of denatured LAAO with the PNGase F results in a Coomassie stained band of higher mobility (≈ 53 kDa) on SDS/PAGE as shown in (Fig. 2A, lane 3). This treatment leads to complete deglycosylation as Schiff's reagent fails to stain the equivalent protein band (Fig. 2B, lane 3). However, when LAAO is treated with PNGase F under nondenaturing conditions, three bands can be distinguished on SDS/PAGE using Coomassie stain (Fig. 2A, lane 2). The lower of the three bands has a mobility equal to that observed with the PNGase F treated denatured protein and is not stained with Schiff's reagent (Fig. 2B, lane 2) while the upper two of these bands are stained with Schiff's reagent (Fig. 2B, lane 2), indicating glycosylation. The electrophoretic mobility of denatured/deglycosylated LAAO indicates a 4–5 kDa lower molecular mass, in agreement with the 3.7-kDa mass difference inferred from ESI-MS measurement of native LAAO (see Fig. 1) and the calculated mass of the protein. Digestion of *C. rhodostoma* LAAO

**Scheme 2. Chemical structure of the dodecasaccharide moiety as deduced by NMR-spectroscopy and mass analysis.** The sugar composition is as follows: a, b, e, and i are *N*-acetylglucosamine residues; c, d, and h are mannose residues; f and j are galactose residues; g and k are *N*-acetylneuraminic acid residues and l is a fucose residue. *R* = α,β-hydroxyl group in the released free oligosaccharide and β-Asn172 and β-Asn361 in the glycoprotein.

free carbohydrate  R = α,β–OH
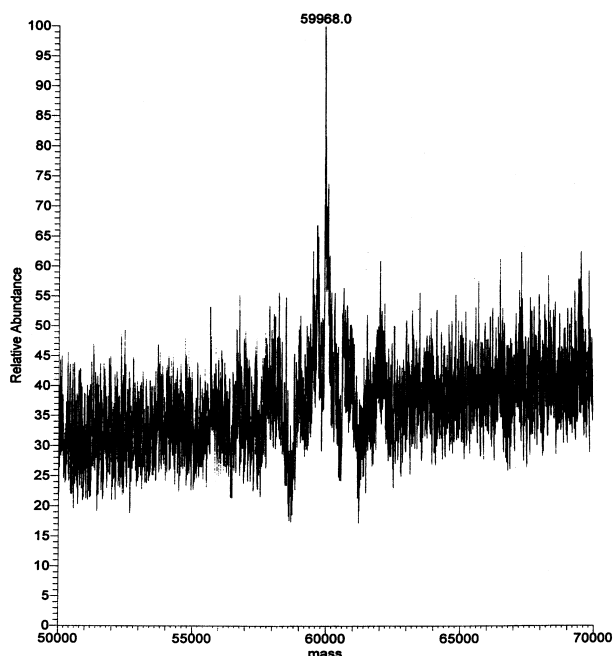N-glycan          R = β-Asn$^{172}$, β-Asn$^{361}$LAAO

**Fig. 1. Electrospray-ionization mass spectrum of native LAAO from *C. rhodostoma*.** The sample was prepared as described in Experimental procedures.



**Fig. 2. Analysis of LAAO deglycosylation by 10% SDS/PAGE.** (A) (Coomassie blue stained) lane 1, untreated native LAAO (1.5 μg protein); lane 2, native LAAO after PNGaseF treatment (3 μg protein); lane 3, denatured LAAO after PNGaseF treatment (3 μg protein). (B) Same as panel A except stained with Schiff's reagent and protein concentrations are 4.5 μg, 9 μg and 6 μg for lanes 1–3, respectively. (C) (Coomassie blue stained) lane 1, untreated native LAAO (2.3 μg protein); lane 2, native LAAO after sialidase treatment (2.3 μg protein).

with Endo $H_f$ and *O*-glycosidase did not affect the mobility of the protein in SDS/PAGE indicating the absence of an N-linked, high mannose structure, and of an O-glycosidic sugar moiety, respectively (data not shown). This result is in agreement with complete removal of the glycan moieties with PNGaseF.

DeKok & Rawitsch have reported the presence of about 1 mol sialic acid per mol FAD for the glycosyl moiety of LAAO from *C. adamanteus* [12] a finding later confirmed by Coles *et al.* [24]. Treatment of the *C. rhodostoma* enzyme with the exoglycosidase sialidase which cleaves sialyl linkages on oligosaccharides results in a slightly higher electrophoretic mobility of the protein (Fig. 2C, compare lanes 1 and 2) indicating the presence of nega-tively charged sialic acid. Further evidence for sialylation of the glycan moiety was obtained by fluorophore-assisted carbohydrate electrophoresis (Fig. 3). The glycan moiety was cleaved off by PNGaseF with and without prior treatment by sialidase and analyzed by PAGE (Fig. 3, lanes 1 and 2, respectively). The higher electrophoretic mobility of the carbohydrate(s) without sialidase treatment indicates the presence of sialic acid. In summary, these findings demonstrate that LAAO contains exclusively N-linked carbohydrates with the distal sugars carrying sialic acid(s). The sugar profile shown in Fig. 3 also demonstrates the prevalence of one glycan moiety of LAAO. This finding encouraged us to isolate the carbohydrate directly from LAAO for elucidation of its structure.

## Isoelectric focusing

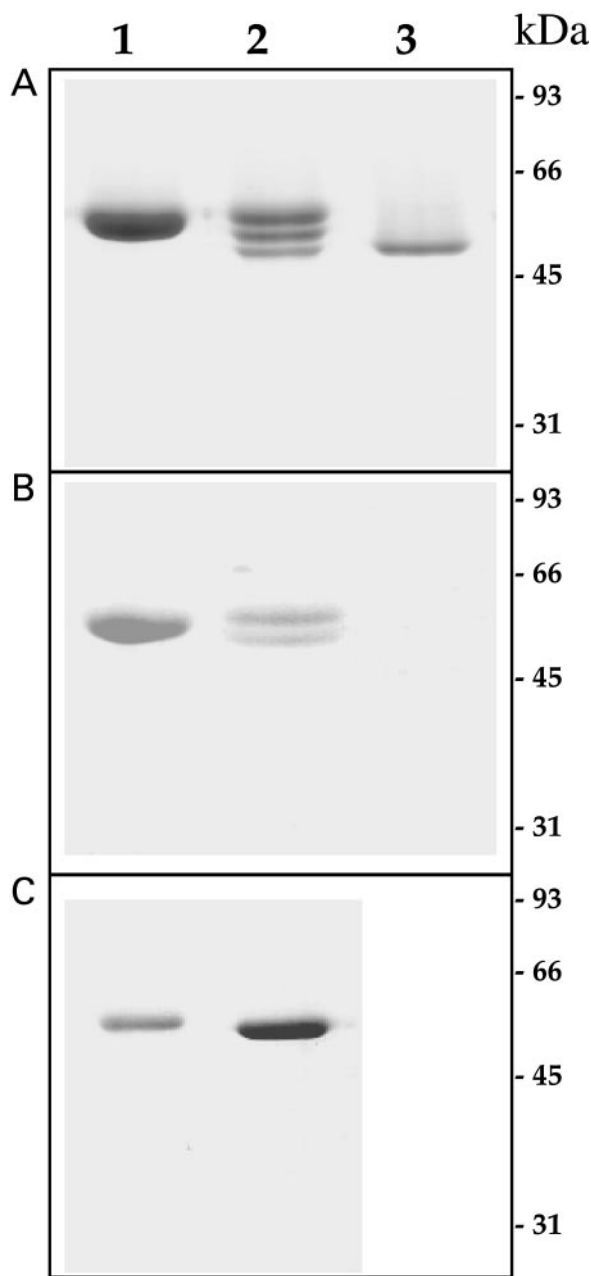Native LAAO subjected to isoelectric focusing using a linear gradient from pH 4–7 shows multiple bands ($\geq$ 8) by Coomassie blue staining indicating a heterogeneous population of this protein (Fig. 4, lane 1). This hetero-geneity appears to be mainly manifested in the glycosylated protein form as complete removal of the sugar moiety, by treating the denatured protein with PNGaseF, results in the appearance of only three bands reflecting different isoforms of the protein moiety itself (Fig. 4, compare lanes 2 and 3). Removal of the sugar also appears to result in the reduction
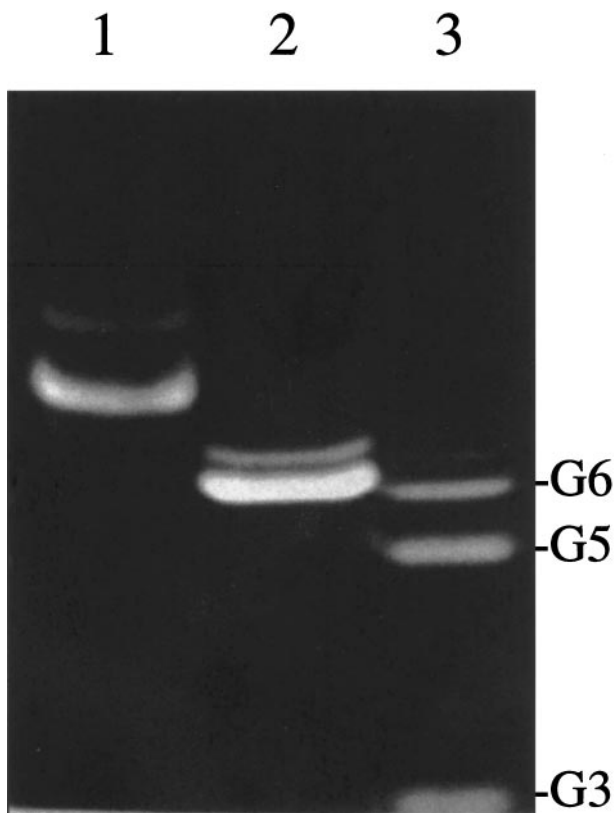
**Fig. 3. Analysis of the sugar content of LAAO by fluorophore-assisted carbohydrate electrophoresis.** Lane 1, PNGase F released and ANTS-labelled carbohydrates after treatment of LAAO with sialidase; lane 2, PNGase F released and ANTS-labelled carbohydrates without prior treatment of LAAO with sialidase and lane 3, glucose ladder (G3,4,5 = three, four and five glucose units, respectively) as provided by the manufacturer (Bio-Rad).

of negative charges on the protein surface as is reflected by its closer mobility towards the cathode. However, treatment of the protein with sialidase results in an even more positively charged protein population as would be predicted by the removal of the negatively charged sialic acid residues (Fig. 4, lane 4). As sialidase treatment of PNGaseF-treated protein (after denaturation) does not alter its mobility (data not shown), it can be concluded that cleavage of N-linked oligosaccharide by PNGaseF leads to (partial) conversion of asparagines to aspartic acid resulting in a diminished mobility in comparison to sialidase treatment alone.

### NMR analysis

Cleavage of the oligosaccharide fraction used for NMR spectroscopy was achieved under nondenaturing conditions with PNGaseF as described in the methods section. During the incubation of LAAO partial denaturation occurred
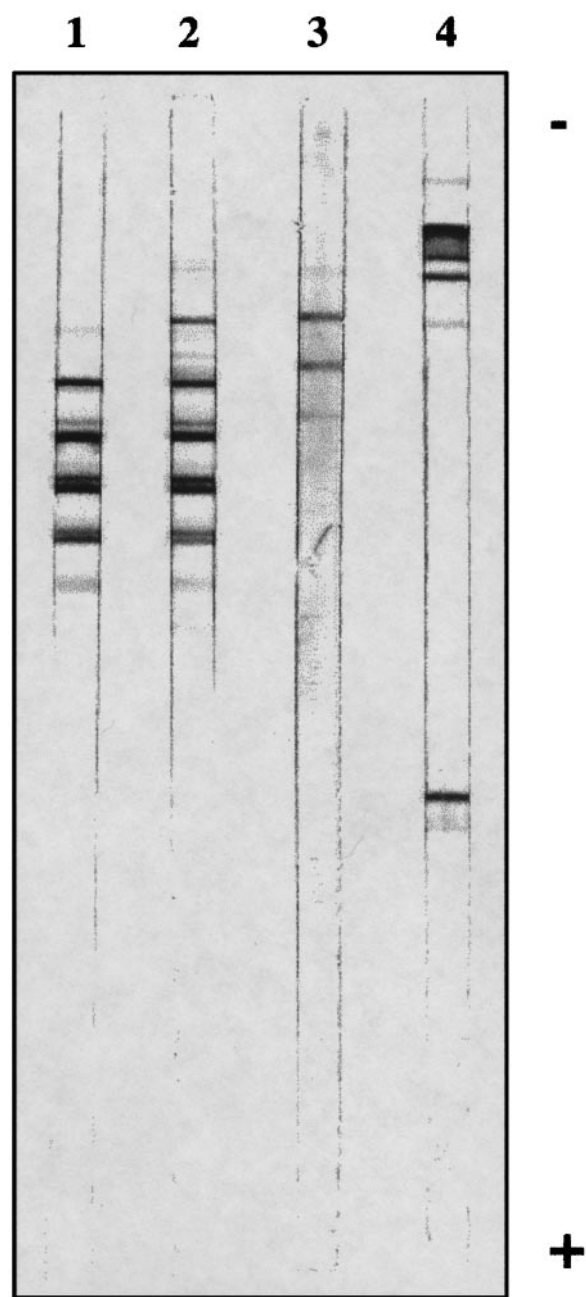


**Fig. 4. Isoelectric focusing experiments with LAAO.** Lane 1, untreated native LAAO; lane 2, native LAAO after PNGaseF treatment; lane 3, denatured LAAO after PNGaseF treatment; lane 4, LAAO after sialidase treatment; (+) and (−) indicate the basic and acidic ends of the IPG strip, respectively,

resulting in release of the FAD-cofactor. The resonance signals of FAD were assigned in the NMR spectra and the anomeric proton of the ribose moiety ($\delta$ 5.85) served as an internal standard for the quantification of the

**Fig. 5. NMR analysis of the oligosaccharide.** Heteronuclear one-bond correlations in the expansion from a HMQC spectrum (top) identify monosaccharides with anomeric CH groups. Vertical lines connect the $^1$H chemical shifts to the expansion from the ROESY spectrum (bottom). Cross signals in the ROESY spectrum are due to short interproton contacts below 0.4 nm. The NOE contacts across glycosidic bonds are highlighted and identify the connectivity of the sugar residues. The two trisaccharide arms e,f,g and i,j,k exhibit identical chemical shifts due to the identical chemical environment, details of the assignment strategy are discussed in the text. The spectra were recorded at 600 MHz (1H) in $D_2O$ (303 K).
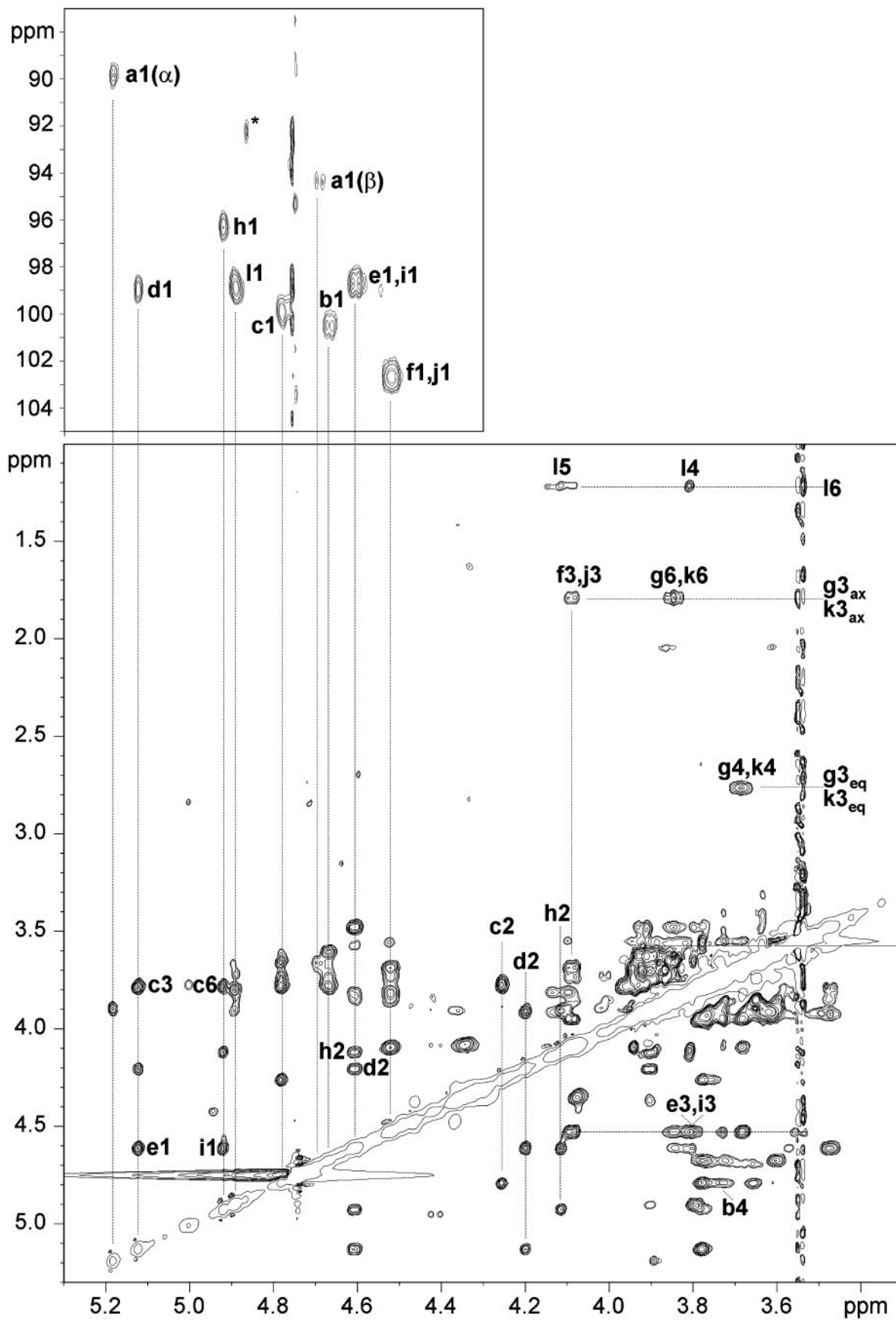
**Table 1. $^1$H and $^{13}$C chemical shifts of the dodecasaccharide moiety depicted in Scheme 2.** The resonance signal assignments are based on the two-dimensional correlation methods described in the experimental part. The numbering of the pyranose rings corresponds to the numbering in Scheme 2. ND = not determined.

|            |          | 1($^1$H) | 1($^{13}$C) | 2    | 3         | 4         | 5    | 6    |
|------------|----------|----------|-------------|------|-----------|-----------|------|------|
| a($\alpha$) | GlcNac $\alpha$ | 5.18 | 89.9 | 3.89 | ND | ND | ND | ND |
| a($\beta$) | GlcNAc $\beta$ | 4.69 | 94.4 | 3.71 | ND | ND | ND | ND |
| b | GlcNAc $\beta$ | 4.67 | 100.4 | 3.79 | 3.73–3.75 | 3.73–3.75 | 3.60 | ND |
| c | Man $\beta$ | 4.78 | 99.9 | 4.25 | 3.78–3.80 | 3.78–3.80 | 3.65 | ND |
| d | Man $\alpha$ | 5.12 | 98.9 | 4.20 | 3.90 | 3.52 | 3.76 | ND |
| e/i | GlcNAc $\beta$ | 4.61 | 98.7 | 3.85 | 3.82 | 3.58 | 3.47 | ND |
| f/j | Gal $\beta$ | 4.52 | 102.7 | 3.54 | 4.09 | 3.94 | 3.68 | ND |
| g/k | Neu5Ac $\alpha$ | – | ND | – | 1.79, 2.76 | 3.68 | 3.63 | 3.84 |
| h | Man $\alpha$ | 4.92 | 96.3 | 4.1 | 3.91 | ND | ND | ND |
| l | Fuc $\alpha$ | 4.89 | 98.9 | 3.80 | 3.94 | 3.81 | 4.12 | 1.22 |

carbohydrate-protein ratio. A ratio of 1.45 : 1 (glycan/FAD) was deduced, which is compatible with the presence of two oligosaccharides per molecule FAD.

A predominant carbohydrate moiety is visible in the $^1$H NMR spectrum, the homogeneity of the estimated 2 mg of carbohydrate is >90%, other protein glycoforms are not detectable. The expansion of the HMQC (Fig. 5, top) identifies the anomeric protons and the corresponding $^{13}$C chemical shifts in the region of δ 100 ($^{13}$C). After enzymatic

cleavage of the β-Asn glycosidic linkage, D-*N*-acetylglucos-amine (GlcNAc) at the reducing terminus of the oligosac-charide (a-GlcNAc in Scheme 2) forms an anomeric mixture. The anomeric proton of the α-anomeric form resonates at δ 5.18 (α-GlcNAc-1Hα), the β-anomeric form is visible at higher field (δ 4.69 p.p.m., α-GlcNAc-1Hβ). This anomeric equilibrium also influences the resonance signals of L-fucose (L-Fuc) and the anomeric proton L-Fuc-1H forms a *pseudo*-triplet at δ 4.89. Doubled integral
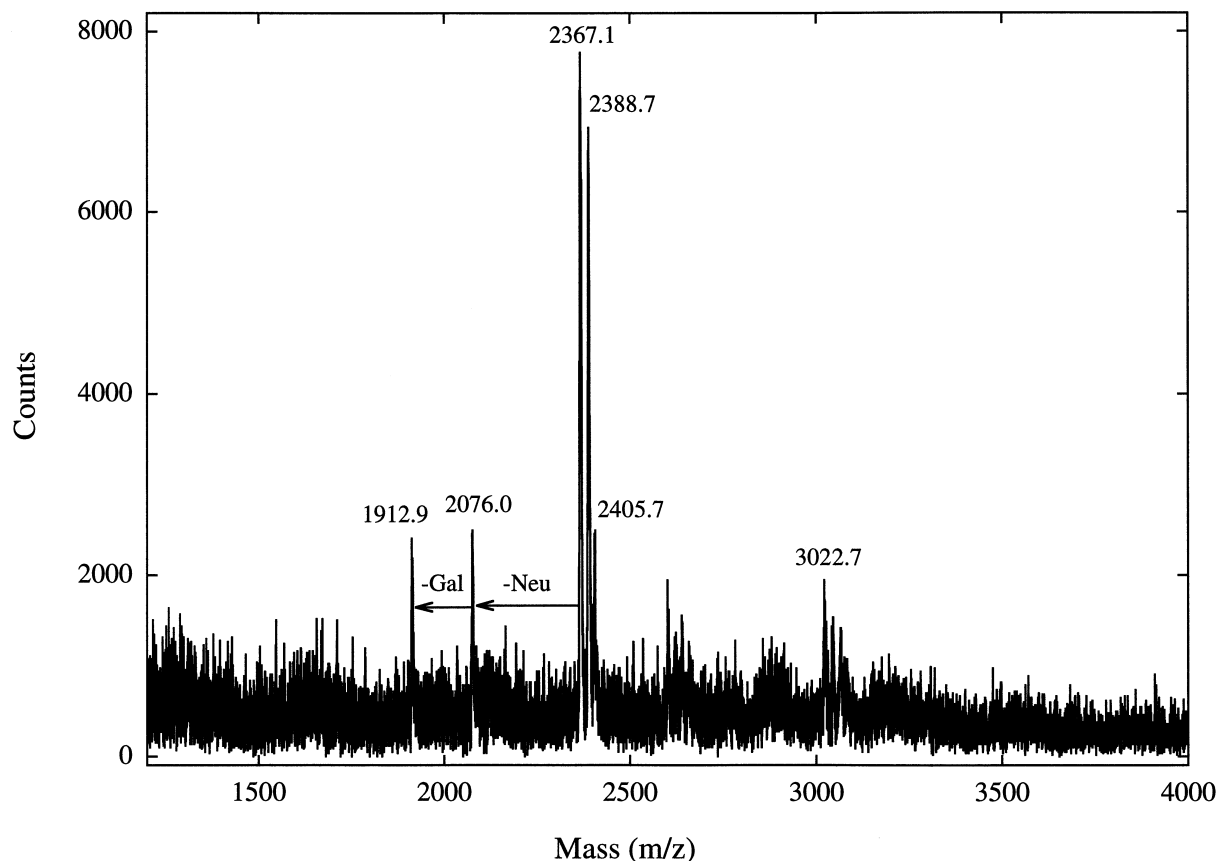


**Fig. 6. MALDI-TOF mass spectrum of the oligosaccharide moiety.** The oligosaccharide(s) were analysed after release from LAAO by PNGaseF as described in Experimental procedures.

intensities were observed for the trisaccharide unit NeuAcα(2–3)Galβ(1–3)Glcβ(1- (where NeuAc = D-*N*-acetylneuraminic acid and Gal = D-galactose) which occurs twice in the oligosaccharide (e,f,g and i,j,k in Scheme 2). Transglycosidic NOE contacts between g,k-NeuAc-3Hax (δ 1.79) and f,j-Gal-3H (δ 4.09) in the expansion from the ROESY spectrum (Fig. 5, bottom) prove the sialylation sites f,j-Gal-O3. The Galβ(1–3)GlcNAc connectivity was identified from the transglycosidic ROE between f,j-Gal-1H and e,i-GlcNAc-3H and from the distinct chemical shift separation of 0.1 p.p.m. of the anomeric protons f,j-Gal-1H and e,i-GlcNAc-1H.

The anomeric protons e,i-GlcNAc-1H (δ 4.61) show cross signals to the anomeric proton of D-mannose (d-Man; δ 5.12) and h-Man (δ 4.92), respectively. The d-Man-1H resonance shows a cross signal to c-Man-3H (δ 3.78), therefore h-Man must be connected to c-Man-O6. The Manβ(1–4)GlcNAc- linkage is identified from the cross signal between c-Man-1H (δ 4.78) and b-GlcNAc-4H (δ 3.72). The chemical shifts of the predominant carbohydrate moiety found in LAAO are summarized in Table 1.

## Mass spectrometric analysis of the sugar moiety of L-amino-acid oxidase

To confirm the structure of the major oligosaccharide and to determine the identity of minor oligosaccharide compounds, samples identical to those utilized for the NMR experiments were analyzed by mass spectrometry. At first, this was attempted by MALDI-TOF mass spectrometry in a DHB matrix. In this matrix a major mass peak at 2014 (MH+) was obtained. However, when the matrix solution was fortified with sodium salts the observed mass varied considerably in the range of 2014–2070 Da. Although DHB is a suitable matrix for neutral sugars it was found to give rise to loss of sialic acid and decarboxylation [17]. Therefore, we analyzed the isolated glycan moiety in a THAP matrix which was found to have excellent properties for the analysis of acidic oligosaccharides [17]. Using this matrix, the mass spectrum shown in Fig. 6 was obtained. The major peak at 2367.1 Da is consistent with the structure of the glycan moiety as determined by NMR spectroscopy (Scheme 2). The masses at 2388.7 Da and 2405.7 Da are for the oligosaccharides carrying one sodium and potassium, respectively, i.e. the MNa⁻ and MK⁻ ions. In addition to these dominant mass peaks, minor peaks at 3022.7 Da, 2076.0 Da, and 1912.9 Da are present in the MALDI-MS-TOF spectrum (Fig. 5). The latter two peaks can be assigned to a biantennary oligosaccharide lacking one sialic acid and one sialic acid and one galactose, respectively, as indicated in Fig. 6. The mass at 3022.7 Da can be assigned to a triantennary oligosaccharide with a third GlcNAc, galactose and sialic acid attached to mannose d or h (theoretical mass = 3025.8 Da; see Scheme 2). As analysis of acidic oligosaccharides under the experimental conditions used reflects their relative abundance [17], it can be safely concluded that the core-fucosylated disialylated biantennary sugar is the major constituent of the glycan moiety (Scheme 2). This result is also in keeping with the prevalence of a major oligosaccharide and at least one minor sugar component as demonstrated by FACE (see Fig. 3).

## DISCUSSION

The data presented here establish unequivocally the structure of the carbohydrate moiety linked to Asn172 and Asn361 of LAAO from *Calloselasma rhodosoma*. The major component is a bis-sialylated, biantennary, core-fucosylated dodecasaccharide (Scheme 2). Our results are consistent with the X-ray structural analysis of the protein which demonstrated the occurrence of sugar residues a, b and l at Asn172 and sugar residue a at Asn361 (see Fig. 7) [13]. The dodecasaccharide shown in Scheme 2 is identical with one of the main glycan moieties identified in ancrod, a serine protease found in *C. rhodostoma* venom [25]. A very surprising finding is the homogeneity of the glycosylation found in *C. rhodostoma* LAAO. Fluorophore-assisted carbohydrate electrophoresis, MALDI-TOF mass spectrometry and NMR-spectroscopy indicate that the major oligosaccharide contributes ≈ 90% of the total glycan substituents. In view of the variability in the relative amount of oligosaccharides in many glycoproteins, the apparent homogeneity in LAAO is rather exceptional. A point in case is provided by the detailed analysis of the glycosylation of ancrod isolated from the same snake species [25]. In this protein biantennary, triantennary and tetraantennary oligosaccharides constitute 23, 40 and 12% of the total glycans, respectively. In addition, more than a dozen of other oligosaccharides occur, contributing around 1% each. In any case, the high homogeneity of the oligosaccharide found in *C. rhodostoma* LAAO may have aided the crystallization of this enzyme [13]. The homogeneity of LAAO glycosylation is perhaps even more surprising as the venom used for isolation of LAAO was collected from some three thousand snake individuals. Isoelectrofocussing of native and deglycosylated LAAO has clearly shown (Fig. 4) that the protein itself is not homogeneous. This finding is in keeping with a recent investigation of the electrophoretic mobility of the components of *C. rhodostoma* venom [26], in which considerable intraspecific variation in many of these proteins, among them LAAO, was shown. Likewise it is conceivable that more than one gene encodes for LAAO as was suspected for *Pseudechis australis* (Australian king brown snake) where two distinct LAAOs were isolated and partially characterized [6]. An interesting possibility with regard to the homogeneity of the glycan moiety is that it is a functional requirement connected with the biological activities ascribed to LAAO, as outlined in the introduction. The last few years have witnessed the discovery of several families of sialic acid-binding lectins, the so-called siglecs (sialic acid-binding Ig superfamily lectins). The nine families of siglecs so far identified in humans are characterized by cell type-specific expression and appear to recognize specific sialic acid motifs [27,28]. The apoptosis-inducing effect of LAAO has been studied with human umbilical cord endothelial, leukemia HL-60 and human ovarian carcinoma (A2780) cells [9]. To our knowledge, no specific siglec has been identified for these cell types and hence it remains to be seen whether this highly interesting family of proteins provide a molecular basis for the understanding of the apoptotic activity of LAAO. As shown in (Fig. 7), the enzyme carries two disialylated oligosaccharides at its surface, one of which (Asn172) is located in direct vicinity to the channel leading to the active site of the enzyme (Fig. 7). Putative binding of LAAO to
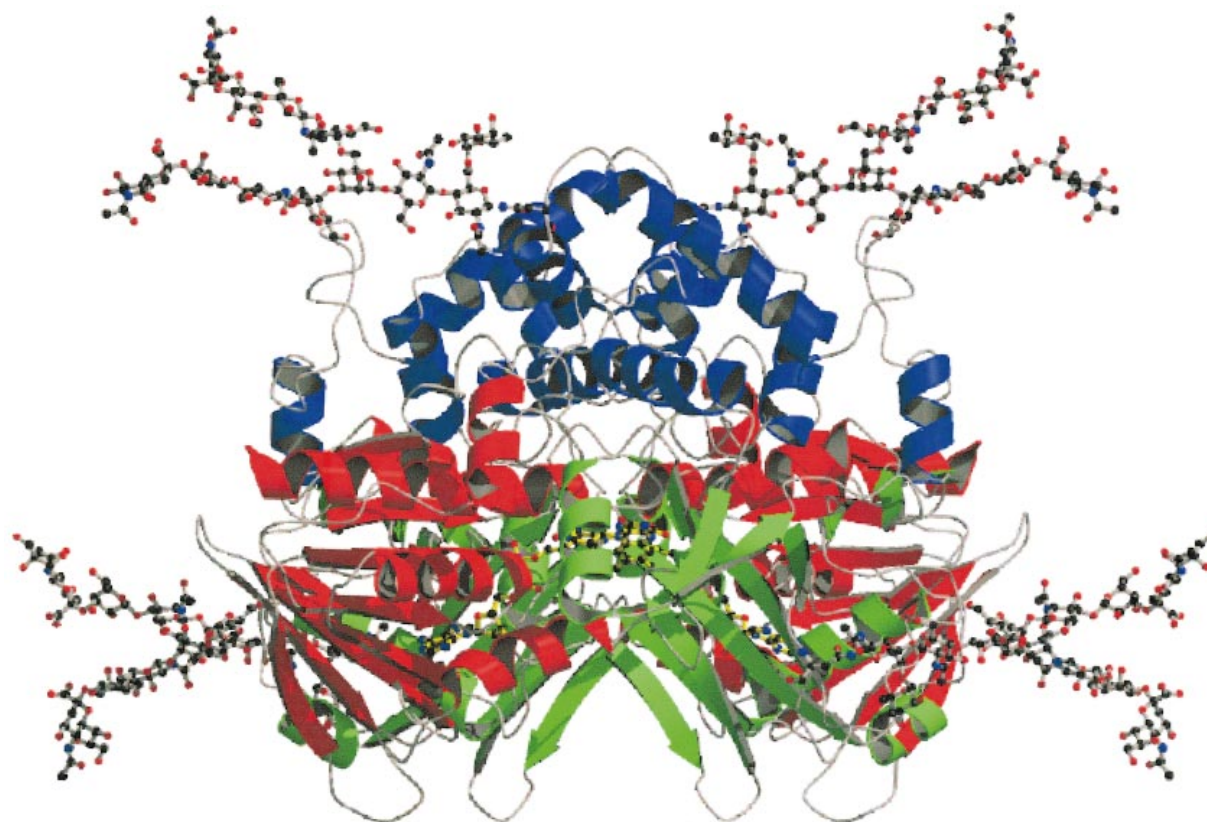
**Fig. 7. Structural model of the dimeric glycoprotein LAAO.** The positional coordinates of the dodecasaccharides were obtained by energy-minimization of averaged conformations of the carbohydrate moiety as described in Experimental procedures. The dodecasaccharide was linked to the glycosylation sites Asn172 and Asn361 based on the published coordinates for *C. rhodostoma* LAAO. The orientation of the Asn side chain as obtained from the X-ray structure was not altered. In aqueous solution the carbohydrate chains populate rotation cones due to the movement dynamics around the side chain torsions of Asn and around glycosidic torsions. Both (1–6) arms probably populate several rotamers of which only one is shown here. Figure created using the computer program MOLSCRIPT [29].

siglecs via its sialylated glycan moiety may then result in production of locally high concentrations of $H_2O_2$ in or near the binding interface; this, in turn, could lead to oxidative damage of the siglec or another adjacent cell structural elements. This scenario is an attractive hypothesis to rationalize the biological effects observed with ophidian LAAO and would support the proposals by Suhr *et al.* [7,8]. The antibacterial activity may proceed via an analogous mechanism. Efforts are under way to assess the role(s) of the glycan moiety of LAAO in more detail by heterologous expression of the ophidian enzyme in a suitable host as well as by enzymatic de-sialylation and deglycosylation of the native enzyme.

# ACKNOWLEDGEMENTS

# REFERENCES

1. Zeller, A.E. (1977) Snake venom action: are enzymes involved in it? *Experientia* **33**, 143–150.

2. Ahn, M.Y., Lee, B.M. & Kim, Y.S. (1997) Characterization and cytotoxicity of L-amino acid oxidase from the venom of king cobra (*Ophiophagus hannah*). *Int. J. Biochem. Cell Biol.* **29**, 911–919.

3. Nathan, I., Dvilansky, A., Yirmiyahu, T., Aharon, M. & Livne, A. (1982) Impairment of platelet aggregation by *Echis colorata* venom mediated by L-amino acid oxidase or $H_2O_2$. *Thromb. Haemost.* **48**, 277–282.

4. Hayes, M.B. & Wellner, D. (1969) Microheterogeneity of L-amino acid oxidase. Separation of multiple components by polyacrylamide gel electrofocusing. *J. Biol. Chem.* **244**, 6636–6644.

5. Skarnes, R.C. (1970) L-amino-acid oxidase, a bactericidal system. *Nature* **225**, 1072–1073.

6. Stiles, B.G., Sexton, F.W. & Weinstein, S.A. (1991) Antibacterial effects of different snake venoms: purification and characterization of antibacterial proteins from *Pseudoechis australis* (Australian king brown or mugla snake) venom. *Toxicon.* **29**, 1129–1141.

7. Suhr, S.-M. & Kim, D.-S. (1996) Identification of the snake venom substance that induces apoptosis. *Biochem. Biophys. Res. Commun.* **224**, 134–139.

8. Suhr, S.M. & Kim, D.S. (1999) Comparison of the apoptotic pathways induced by L-amino acid oxidase and hydrogen peroxide. *J. Biochem. (Tokyo).* **125**, 305–309.

9. Torii, S., Naito, M. & Tsuruo, T. (1997) Apoxin I, a novel apoptosis-inducing factor with L-amino acid oxidase activity purified from Western diamondback rattlesnake venom. *J. Biol. Chem.* **272**, 9539–9542.

10. Torii, S., Yamane, K., Mashima, T., Haga, N., Yamamoto, K., Fox, J.W., Naito, M. & Tsuruo, T. (2000) Molecular cloning and functional analysis of apoxin I, a snake venom-derived apoptosis-inducing factor with L-amino acid oxidase activity. *Biochemistry* **39**, 3197–3205.

11. Curti, B., Ronchi, S. & Pilone Simonetta, M. (1992) D- and L-amino acid oxidases. *Chemistry and Biochemistry of Flavo-enzymes* (Müller, F., ed.), pp. 69–94. CRC Press, Boca Raton, FL, USA.

12. deKok, A. & Rawitch, A.B. (1969) Studies on L-amino acid oxidase. II. Dissociation and characterization of its subunits. *Biochemistry.* **8**, 1405–1411.

13. Pawelek, P., Cheah, J., Coulombe, R., Macheroux, P., Ghisla, S. & Vrielink, A. (2000) The structure of L-amino acid oxidase reveals the substrate trajectory into an enantiomerically conserved active site. *EMBO J.* **19**, 4204–4215.

14. Macheroux, P., Seth, O., Bollschweiler, C., Schwarz, M., Kurfürst, M., Au, L.-C. & Ghisla, S. (2001) L-Amino acid oxidase from the Malayan pit viper *Calloselasma rhodostoma*: comparative sequence analysis and characterization of active and inactive forms of the enzyme. *Eur. J. Biochem.* **268**, 1679–1686.

15. Laemmli, U.K. (1970) Cleavage of structural proteins during the assembly of the head of bacteriophage T4. *Nature (London)* **227**, 680–685.

16. Jay, G.D., Culp, D.J. & Jahnke, M.R. (1990) Silver staining of extensively glycosylated proteins on sodium dodecyl sulfate-polyacrylamide gels: enhancement by carbohydrate-binding dyes. *Anal. Biochem.* **185**, 324–330.

17. Papac, D., Wong, A. & Jones, A.J.S. (1996) Analysis of acidic oligosaccharides and glycopeptides by matrix-assisted laser desorption/ionization time-of-flight mass spectrometry. *Anal. Chem.* **68**, 3215–3223.

18. Braunschweiler, L. & Ernst, R.R. (1983) Coherence transfer by isotropic mixing – application to protein correlation spectroscopy. *J. Magn. Reson.* **53**, 521–528.

19. Piantini, U., Sörensen, O.W. & Ernst, R.R. (1982) Multiple quantum filters for elucidating NMR coupling networks. *J. Am. Chem. Soc.* **104**, 6800–6801.

20. Müller, L. (1979) Sensitivity enhanced detection of weak nuclei using heteronuclear multiple quantum coherence. *J. Am. Chem. Soc.* **101**, 4481–4484.

21. Bothner-By, A.A., Stephenson, R.L., Lee, J., Warren, C.D. & Jeanloz, R.W. (1984) Structure determination of a tetrasaccharide: transient nuclear Overhauser effects in the rotating frame. *J. Am. Chem. Soc.* **106**, 811–813.

22. Griesinger, C. & Ernst, R.R. (1987) Frequency offset effects and their elimination in NMR rotating-frame cross-relaxation spectro-scopy. *J. Magn. Reson.* **75**, 261–271.

23. Woods, R.J., Pathiaseril, A., Wormald, M.R., Edge, C.J. & Dwek, R.A. (1998) The high degree of internal flexibility observed for an oligomannose oligosaccharide does not alter the overall topology of the molecule. *Eur. J. Biochem.* **258**, 372–386.

24. Coles, C.J., Edmondson, D.E. & Singer, T.P. (1977) Reversible inactivation of L-amino acid oxidase. Properties of the three conformational forms. *J. Biol. Chem.* **252**, 8035–8039.

25. Pfeiffer, G., Dabrowski, U., Dabrowski, J., Stirm, S., Strube, K.-H. & Geyer, R. (1992) Carbohydrate structure of a thrombin-like serine protease from *Agkistrodon rhodostoma*. Structure elucida-tion of oligosaccharides by methylation analysis, liquid secondary-ion mass spectrometry and proton magnetic resonance. *Eur. J. Biochem.* **205**, 961–978.

26. Daltry, J.C., Ponnudurai, G., Shin, C.K., Tan, N.H., Thorpe, R.S. & Wuster, W. (1996) Electrophoretic profiles and biological activities: intraspecific variation in the venom of the Malayan pit viper (*Calloselasma rhodostoma*). *Toxicon.* **34**, 67–79.

27. Angata, T. & Varki, A. (2000) Cloning, characterization, and phylogenetic analysis of Siglec-9, a new member of the CD33-related group of Siglecs. *J. Biol. Chem.* **275**, 22127–22135.

28. Brinkman-Van der Linden, E.C.M. & Varki, A. (2000) New aspects of Siglec binding specificities, including the significance of fucosylation and of the sialyl-Tn epitope. *J. Biol. Chem.* **275**, 8625–8632.

29. Kraulis, P. (1991) MOLSCRIPT: a program to produce both detailed and schematic plots of protein structures. *J. Appl. Crystallogr.* **24**, 946–950.